PERGAMON

Chemical Engineering Science 55 (2000) 2143–2150

Chemical Engineering Science

Alternative designs for a catalytic converter operating under autothermal conditions

Eduardo López, Alberto F. Errazu, Daniel O. Borio, Verónica Bucalá*

Planta Piloto de Ingeniería Química, UNS-CONICET, Camino ha, Garrindanga Km7, (8000) Bahía Blanca, Argentina

Received 11 February 1999; accepted 17 August 1999

Abstract

This paper focuses on the study of two different autothermal designs of a catalytic combustor, based on natural gas oxidation for heat generation. The feed is preheated by means of two different alternatives: (a) indirect heat exchange between the products and feed streams (Design I), (b) direct heat exchange by recycling a fraction of the hot gases leaving the catalytic combustor (Design II). Steady-state and dynamic results have demonstrated that autothermal catalytic units, after an appropriate start-up procedure, can operate with high methane conversion, without exceeding the maximum allowable temperature and minimizing harmful emissions such as NO_x (to preheat the reactants, the flame of conventional units is replaced by a heat feedback of a fraction of the total heat generated by the catalytic combustor). Due to the dilution originated by the recycle stream (which admits the use of higher methane molar fractions in the fresh feed stream) Design II appears as the most convenient alternative because it can provide significantly higher heat fluxes than Design I for the same process constraints. Moreover, Design II can provide an exit stream at the highest thermal level (for a given maximum allowable temperature) feasible for an autothermal converter.

Keywords: Catalytic combustion; Monolith; Autothermal reactor; Catalytic combustor

1. Introduction

Catalytic combustion is being adopted for different industrial and domestic applications. This type of combustion is gradually replacing the homogeneous (conventional) one because it offers attractive features, among others, flameless operation, lower emissions of contaminants, lower operating temperatures (Hayes & Kolaczkowski, 1997). The catalytic combustion processes can be grouped into those for heat generation (primary combustion) and those for streams purification (secondary combustion). Stationary gas turbines, radiant heaters, process fluids heaters are examples of catalytic combustors for heat generation, while catalytic converters for gasoline and diesel engines, catalytic incineration of organic contaminants represent secondary combustion processes.

There are several types of reactors to carry out catalytic combustion. The multichannel monoliths is being widely used because, among other reasons, operates with low pressure drop and high surface/volume ratio and minimizes gas channeling due to the uniformity of the matrix (Hayes & Kolaczkowski, 1997). Cybulski and Moulijn (1994,1998), Irandoust and Andersson (1988), Hayes and Kolaczkowski (1997), Groppi, Tronconi and Forzatti (1993), among others, have reported different applications of catalytic combustion in monolithic structures.

Natural gas is a common fuel for heat generation. Particularly, the catalytic combustion of methane over Pd/Al_2O_3 catalysts has been extensively studied (Chaouki, Guy, Sapundzhiev, Kusohorsky & Klvana, 1994; Ribeiro, Chow & Dalla Betta, 1993; Briot & Primet, 1991; among others). Kolaczkowski, Thomas, Titiloye and Worth (1996) have analyzed this reaction in a monolith structure with a $Pd/\gamma\text{-}Al_2O_3$ catalyst and steady-state mathematical models of different complexity to obtain a good match between experimental and theoretical results. Dynamic studies of methane combustion in a monolith reactor have been done by Hayes, Kolaczkowski, Thomas and Titiloye (1996).

* Corresponding author. Tel.: 001-54-291-4861700; fax: 001-54-291-4861600.

E-mail addresses: edulopez@criba.edu.ar (E. López), rebucala@criba.edu.ar (V. Bucalá)

0009-2509/00/$ - see front matter
PII: S0009-2509(99)00477-7

Nomenclature

a_v	external (superficial) surface area, m^2/m^3
C	concentration, $gmol/m^3$
cp	specific heat, J/Kg K
$\overline{cp}$	average specific heat, J/Kg K
d	channel hydraulic diameter, m
E_a	activation energy, J/gmol
F	specific molar flowrate, $gmol/m^2$ s
G	specific mass flowrate, Kg/m^2 s
h	heat transfer coefficient (gas–solid), W/m^2 K
k_∞	preexponential factor, $gmol/m^2$ s
k_c	mass transfer coefficient, m/s
R	universal gas constant, J/gmol K
T	temperature, K
t	time, s
x	conversion
y	molar fraction
z	axial coordinate, m

Greek letters

ΔH	heat of reaction, J/gmol
ΔT_{ad}^R	$(-\Delta H)y_{A0}/\overline{cp}$, adiabatic temperature rise in the monolithic reactor, K
ΔT_{ad}	$(-\Delta H)y_{Af}/\overline{cp}$, adiabatic temperature rise in the autothermal converter, K
ε	monolith porosity
η	effectiveness factor
λ	recycle ratio (see Fig. 1)
ρ	density, Kg/m^3

Subscripts

0	at the reactor inlet ($z = 0$)
A	methane
e	at the autothermal converter exit
f	fresh feed
g	gas phase
i	initial (at $t = 0$)
ig	ignition
L	at the reactor outlet ($z = L$)
ma	maximum allowable
s	solid phase

Superscripts

I	Design I
II	Design II

If the fuel/air mixture is available at room temperature, it should be preheated up to the temperature for which the catalytic reaction begins. To reach high conversion levels in a catalytic reactor (Pd/γ-Al_2O_3 as catalyst) of a reasonable length, the inlet temperature has to be much higher than room temperature (approximately $> 300^\circ C$, depending on the design and operating parameters). Therefore, the reactants preheating is indispensable in order to operate the catalytic combustor.

Homogeneous combustion is widely employed to preheat the reactant mixture, in fact, a preburner is commonly used in practice to reach the temperature where catalytic oxidation begins (Cybulski & Moulijn, 1998; Kirchner & Eigenberger, 1997). However, the homogeneous combustion contributes to generate NO_x, which are harmful for the environment. Despite the NO_x can be reduced downstream in the catalytic combustor, a better alternative is to eliminate the preburner and to preheat the feed in flameless conditions (Cybulski & Moulijn, 1998). An autothermal operation, where the feed stream is preheated by means of a fraction of the total amount of heat generated in the catalytic combustor, appears as an attractive alternative.

This paper focuses on the study of two different autothermal designs of a catalytic combustor based on natural gas oxidation for heat generation. The heat feedback, inherent to all autothermal processes, is a source of reactor instability due to the existence of multiple steady states associated with ignition–extinction phenomena. Therefore, these systems have to be carefully designed to operate the reactor at a stable steady state, with high fuel conversion (low emissions of unburned hydrocarbons) and without surpassing the maximum allowable temperature (to avoid irreversible catalyst damages). The proposed designs are studied and compared by means of steady-state and dynamic simulations.

2. Main features of the proposed designs

Two different autothermal catalytic reactors for methane combustion are studied in this paper. These converters have been designed in order to satisfy the following constraints:

- Low pressure drop. A monolithic structure has been selected to satisfy this requirement.
- Adiabatic reactor.
- High methane conversion to minimize emissions of contaminants.
- Maximum allowable temperature (gas and solid phases) lower than $650^\circ C$ to prevent the deactivation of the Pd/γ-Al_2O_3 catalyst.

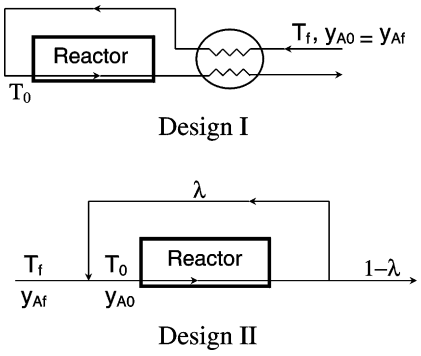

Fig. 1. Autothermal designs for generation of hot gases.

- Autothermal operation.
- Low heat flux (domestic scale).

In addition to the above-mentioned characteristics, a single and adiabatic monolith was considered aiming to a simple and compact design.

Fig. 1 shows schemes of the catalytic converters studied in the present work. In Design I the feed is preheated in an external heat exchanger, by using the hot gases leaving the reactor (indirect heat transfer). A countercurrent (double-pipe type) heat exchanger has been selected.

The second design (Design II) solves the preheating problem by mixing the cold feed with a recycle of hot exhaust gases generated in the catalytic unit (simultaneous mass and heat feedback).

3. Mathematical model of the monolith reactor

A dynamic one-dimensional heterogeneous plug-flow model has been used to represent the behavior of the reactor. According to Cybulski and Moulijn (1994) the axial dispersion effect can be neglected for gas-phase reaction in monolith structures. The adiabatic operation and the uniformity of the ceramic matrix (relatively equal channels) justifies the use of a one-dimensional model. A heterogeneous model is chosen to take into account the concentrations and temperature gradients between the solid and gas phases. These gradients can be very important when the chemical reaction becomes very fast (Kolaczkowski et al., 1996).

The reaction rate expression for methane combustion reported by Kolaczkowski et al. (1996) was used for the simulations.

The mass and energy balances for gas and solid phases are the following:

Gas phase:

$$\frac{\partial C_{A,g}}{\partial t} = -\frac{\partial F_{A,g}}{\partial z} - \frac{4k_c}{d}(C_{A,g} - C_{A,s}), \tag{1}$$

$$\frac{\partial T_g}{\partial t} = -\frac{G}{\rho_g}\frac{\partial T_g}{\partial z} + \frac{4h}{d\rho_g cp_g}(T_s - T_g). \tag{2}$$

Solid phase:

$$\frac{\partial C_{A,s}}{\partial t} = \frac{a_v k_c}{(1-\varepsilon)}(C_{A,g} - C_{A,s}) - \frac{a_v}{(1-\varepsilon)}\eta k_\infty \exp\left[\frac{-E_a}{RT_s}\right] y_{A,s}^{0.72} \tag{3}$$

$$\frac{\partial T_s}{\partial t} = -\frac{a_v h}{(1-\varepsilon)\rho_s cp_s}(T_s - T_g) + \frac{a_v}{(1-\varepsilon)\rho_s cp_s}(-\Delta H)\eta k_\infty \exp\left[\frac{-E_a}{RT_s}\right] y_{A,s}^{0.72}. \tag{4}$$

The initial and boundary conditions used to solve the proposed model are

$T_g = T_s = T_i, \quad t = 0$ all z values,

$C_{A,s} = C_{A,g} = 0, \quad t = 0$ all z values,

$T_g = T_0, \quad z = 0, \quad t > 0,$

$C_{A,g} = C_{A_0}, \quad z = 0, \quad t > 0.$

The heat and mass transfer coefficients between the gas and the channel walls were evaluated using expressions reported by Hawthorn (1974). For all axial positions, the internal temperature gradients (in the washcoat) were neglected. The internal resistance for mass transfer was taken into account by means of the effectiveness factor (η), which was evaluated following the guidelines given by Leung, Hayes and Kolaczkowski (1996), Kolaczkowski et al. (1996) and Hayes and Kolaczkowski (1997). The pressure drop in the monolith reactor was neglected for modeling purposes. The physical properties of the gas mixture were assumed to be dependent on temperature and composition.

To solve the dynamic model, the axial coordinate was discretized using fourth-order backward finite differences. Integration in time of the resulting ODE were performed by means of a Gear algorithm. The steady-state model can be obtained if the left-hand side of Eqs. (1)–(4) are assumed to be zero. This set of differential-algebraic equations was solved using a Backward-Difference Formula (BDF algorithm).

4. Steady-state results: comparison of the proposed designs

In what follows, the steady-state operations of Designs I and II are compared. For this comparison the following variables have been kept constant:

- *Maximum allowable temperatures for gas and solid phases* ($T_{ma} \leqslant 650^\circ$C).

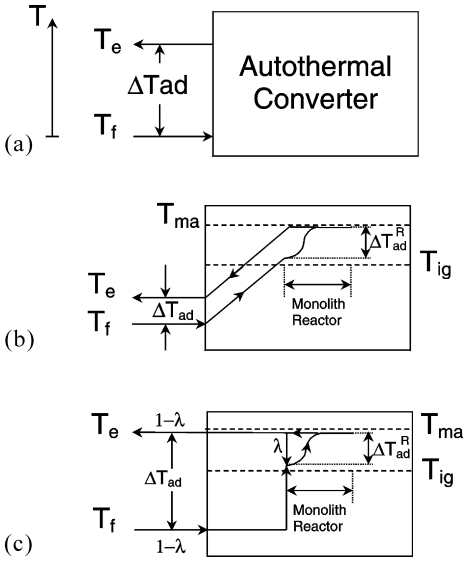

Fig. 2. Schematic conceptualization of the proposed autothermal designs (complete conversion is assumed).

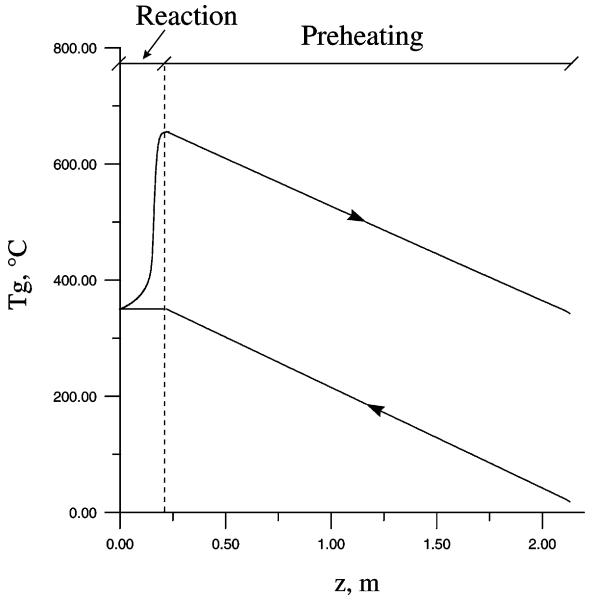

Fig. 3. Axial gas temperature profiles for Design I ($y_{A0} = 0.012$). Dimensions of the double-pipe heat exchanger: internal diameter = 1/2″, external diameter = 3/4″, tube number = 9, tube length = 1.91 m.

- *Reactor dimensions* (length = 0.22 m, reactor diameter = 0.117 m, channels 0.001 m, square).
- *Feed mass flowrate* (0.03 kg/s).

Fig. 2 shows a schematic representation of the proposed autothermal units. By applying the global energy balance to the whole autothermal system (Fig. 2a), the feed and exit temperatures are related by the following equation:

$$T_e = T_f + \Delta T_{\mathrm{ad}} x_A \tag{5}$$

where

$$\Delta T_{\mathrm{ad}} = (-\Delta H) y_{Af} / \overline{cp} \tag{6}$$

Operating at conditions of complete conversion, the maximum allowable feed methane fraction can be calculated from Eq. (5) by setting $T_e = T_{ma}$:

$$(y_{Af})_{ma} = (T_{ma} - T_f)\overline{cp}/(-\Delta H). \tag{7}$$

For methane combustion and assuming $T_{ma} = 650^{\circ}\mathrm{C}$ and $T_f = 20^{\circ}\mathrm{C}$ (room temperature), from Eq. (7) the autothermal unit should operate with a y_{Af} lower than approximately 2.5%.

In an analogous way the inlet and outlet temperatures of the monolith reactor can be related by

$$T_L = T_0 + \Delta T_{\mathrm{ad}}^R x_A, \tag{8}$$

where ΔT_{ad}^R is the adiabatic temperature rise within the reactor, which is defined by

$$\Delta T_{\mathrm{ad}}^R = (-\Delta H) y_{A0} / \overline{cp}. \tag{9}$$

T_0 has to be higher than the ignition temperature (T_{ig}) in order to achieve complete conversion. In addition, to improve the converter performance the reactor exit temperature should be close to T_{ma}. Taking into account the above considerations, the maximum allowable methane fraction at the reactor entrance can be expressed as

$$(y_{A0})_{ma} = (T_{ma} - T_{\mathrm{ig}})\overline{cp}/(-\Delta H). \tag{10}$$

Assuming $T_{ma} = 650^{\circ}\mathrm{C}$ and T_{ig} close to 350°C, the monolith converter can handle up to a methane fraction of 1.2% at the reactor entrance. The constraints given by Eqs. (7) and (10) must be satisfied simultaneously for any autothermal design.

To illustrate the operation of Design I, Fig. 3 shows the axial gas temperature profiles at the monolith (reaction zone) and the heat exchanger (preheating zone). For this example, the feed stream with a methane fraction of 1.2% enters the heat exchanger at 20°C (T_f) and it is preheated up to the reaction temperature ($T_{\mathrm{ig}} = 350^{\circ}\mathrm{C}$). Methane conversion near completion is achieved in the monolith leading to an adiabatic temperature rise approximately of 300°C (ΔT_{ad}^R). The hot gases leave the reactor around 650°C and are available at about 343°C (T_e) after preheating the feed.

It is well known that the heat feedback towards the reactor inlet is a source of instability. Fig. 4 shows the s-shaped curves of outlet reactor temperature vs. T_f, for different feed compositions. In fact, up to three different steady states exist for the same inlet conditions. However, to achieve almost complete methane conversion, the

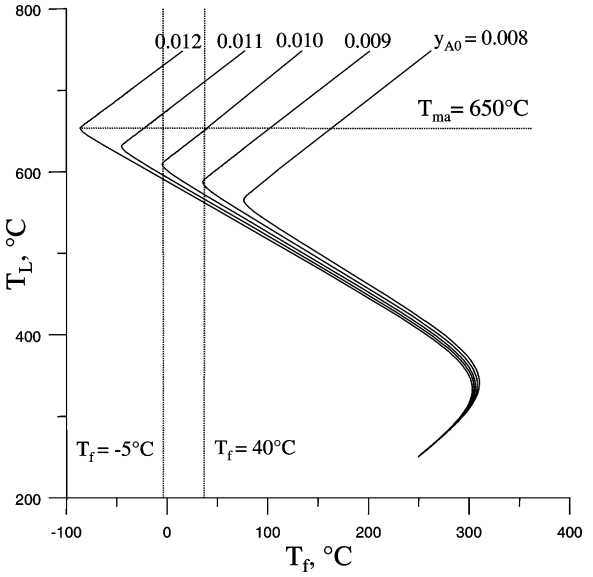

Fig. 4. Design I: outlet gas temperature as affected by the feed temperature for different methane fractions in the feed stream. Dimensions of the double-pipe heat exchanger: internal diameter = 1/2″, external diameter = 3/4″, tube number = 9, tube length = 2.5 m.

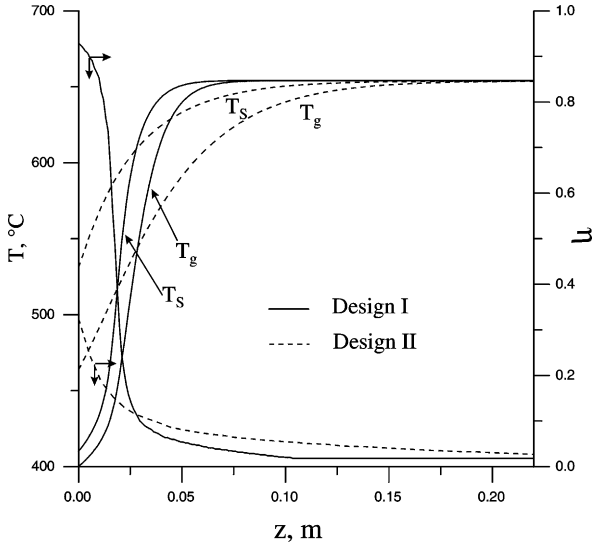

Fig. 5. Axial gas and solid temperature profiles and effectiveness factor for Designs I and II. Design I: $y_{Af} = y_{A0} = 0.010$, $T_0 = 400°C$, $x_A = 0.999$; Design II: $\lambda = 0.7$, $y_{Af} = 0.025$, $y_{A0} = 0.0075$, $T_f = 20°C$, $x_A = 0.997$.

system has to be operated at the upper branches of the curves shown in Fig. 4. For the selected heat exchanger, the extinction temperatures vary from 80°C (for $y_{A0} = 0.008$) to $-80°C$ (for $y_{A0} = 0.012$). Therefore, for the usual room temperatures (e.g., $-5 < T_f < 40°C$) the system can work either in an operating zone where three steady states occur or at a steady state of negligible conversion (for T_f lower than the extinction temperature). As it can be seen in Fig. 4, the extinction temperatures diminish as y_{A0} increases, however y_{A0} cannot surpass $(y_{A0})_{ma}$ (see Eq. (10)).

For the usual room temperatures (e.g., $-5 < T_f < 40°C$) the feasible range for the inlet methane fraction is $0.009 < y_{A0} < 0.012$. y_{A0} values lower than 0.9% are not feasible because the system cannot be operated with complete conversion. On the other hand, y_{A0} values higher than 0.012 violate Eq. (10). For the expected T_f values and inlet methane fractions of 0.011 and 0.012, T_L exceeds $T_{ma} = 650°C$ (see Fig. 4). This problem could be solved if a fraction of the cold feed bypasses the heat exchanger, leading to a decrease in T_0 and consequently in T_L.

For both designs, the gas and solid temperatures and the effectiveness factors along the axial coordinate of the monolith are presented in Fig. 5. These results indicate the need to take into account the effect of both external and internal transport resistance. In fact, the effectiveness factors show a steep drop close to the reactor entrance (mainly Design I) and low values along most of the reactor. The differences between the gas and solid temperatures are high, particularly around 80°C at axial positions where the reaction rate reaches its maximum value.

For Design II and the operating conditions of Fig. 5, the reactants stream enters the reactor at around 460°C (T_0). This inlet temperature is reached by mixing the 70% of the hot exhaust gases (at 650°C) with the fresh feed ($T_f = 20°C$). Besides preheating, the recycle stream dilutes the feed, therefore Design II can handle higher feed methane fractions (without surpassing T_{ma}) than those allowable for Design I. For the examples illustrated in Fig. 5, both designs reach the maximum allowable temperature using very different values of y_{Af} (i.e., $y_{Af} = 1\%$ for Design I, and $y_{Af} = 2.5\%$ for Design II). Since the total mass flowrate is kept constant and almost complete conversion can be achieved, Design II can generate a significantly higher amount of heat than Design I (for conditions of Fig. 5, Design II can increase 2.5 times the heat generated by Design I).

The autothermal operation given by Design II may also lead to multiple steady states due to the heat feedback caused by the recycle stream. Up to three different steady states may exist for the same operating conditions. For different y_{Af}, Fig. 6 shows steady states of high (solid line) and intermediate (broken line) methane conversions. For the operating conditions of Fig. 6, a third branch corresponding to extinguished steady states (negligible conversion) exists, which should be avoided for practical applications.

Design II operating with $T_f = 20°C$ and $y_{Af} = 0.025$ leads to almost complete methane conversion without surpassing 650°C for a wide range of recycle ratios (0.55–0.77, see Fig. 6). The value of $\lambda = 0.7$ has been selected in order to: (a) prevent the extinction of the reactor if any negative disturbance in y_{Af} or λ occurs,

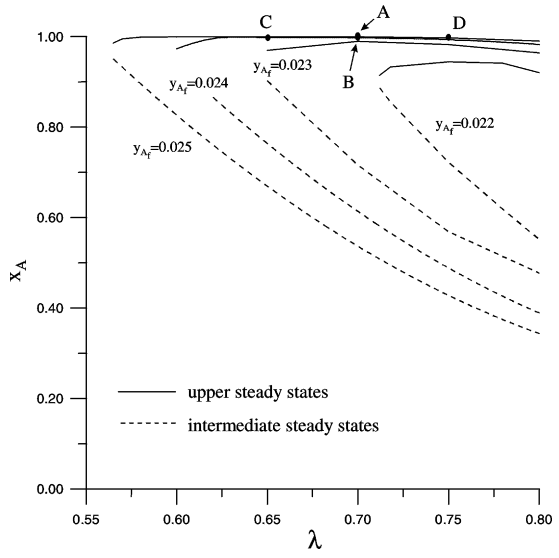

Fig. 6. Design II: methane conversion as affected by the recycle ratio (λ) for different feed methane fractions ($T_f = 20°C$).

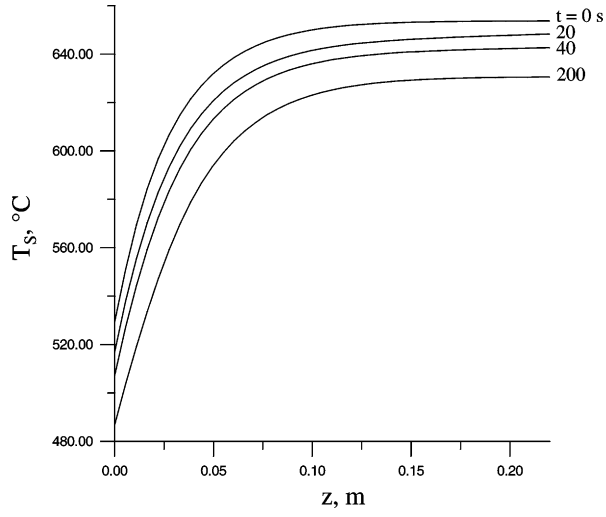

Fig. 7. Dynamic evolution of the axial solid temperature for a step change in y_{Af} (from 0.025 to 0.024), $T_f = 20°C$ and $\lambda = 0.7$.

and (b) to avoid high pressure drops originated by higher recycle ratios (for the selected operating conditions the calculated pressure drop is around 6 KPa).

Independently of the chosen value of maximum allowable temperature, Design II would provide higher energy fluxes than Design I. Since for Design I $y_{Af} = y_{A0}$ the adiabatic temperature rises for the whole autothermal system and for the monolith reactor become coincident (see Eqs. (6) and (9), and Fig. 2b). Particularly if $y_{A0} = (y_{A0})_{ma}$ and complete conversion is achieved, the adiabatic temperature rise for the autothermal converter can be expressed as

$$(\Delta T_{\mathrm{ad}})^{\mathrm{I}}_{ma} = (\Delta T^{R}_{\mathrm{ad}})^{\mathrm{I}}_{ma} = T_{ma} - T_{\mathrm{ig}}. \tag{11}$$

From Eqs. (6) and (7), the maximum allowable temperature rise for Design II becomes

$$(\Delta T_{\mathrm{ad}})^{\mathrm{II}}_{ma} = T_{ma} - T_f. \tag{12}$$

Since $T_f < T_{\mathrm{ig}}$, the maximum temperature rise of Design II is higher than that of Design I whatever is the T_{ma} value.

The dilution of the feed given by the recycle stream of Design II allows to operate the system with higher feed methane fractions, and consequently higher ΔT_{ad} and higher heat production rates than Design I. Furthermore, Design II can provide an exit stream at the highest thermal level allowable for the autothermal converter.

Although Design II presents very interesting features, the dynamic of this system has to be studied to evaluate its stability and define appropriate start-up procedures.

5. Dynamic studies for Design II

5.1. Effects of operating variables disturbances on the dynamic behavior of Design II

Fig. 7 shows the dynamic evolution of the axial solid temperature profile for a step change of y_{Af} from 0.025 to 0.024. The initial steady state (point A of Fig. 6) tends to a new one of lower outlet temperature (which corresponds to point B of Fig. 6). Although a negative step change of 4% in y_{Af} occurs, the system maintains a similar conversion level (near completion).

Fig. 8 presents the dynamic evolution of the axial solid temperature for a negative step change in λ. The initial steady state ($\lambda = 0.7$) corresponds to point A of Fig. 6, while the final steady state ($\lambda = 0.65$) is the point labeled as C in the same figure. This step change in λ causes a higher reactor residence time, lower inlet gas temperature (T_0), and higher inlet methane molar fraction (y_{A0}) due to the decrease of the recycle mass flowrate. All these effects tend to offset each other and lead to almost the same outlet values of conversion and temperature than those of the initial steady state (see Figs. 6 and 8). An increase in λ, for example from 0.7 to 0.75 (the steady state of point A moves to point D in Fig. 6) causes lower reactor residence time, higher T_0, and lower y_{A0}. As it happens for negative λ steps, the outlet conditions also remain almost invariant.

Dynamic studies have also demonstrated that the steady state called A in Fig. 6 shows low sensitivity with respect to disturbances in T_f and feed mass flowrate.

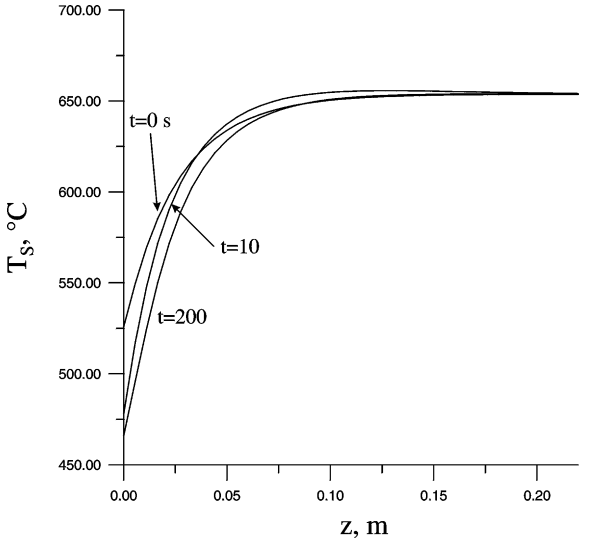

Fig. 8. Dynamic evolution of the axial solid temperature for a step change in λ (from 0.7 to 0.65), $T_f = 20°C$ and $y_{Af} = 0.025$.

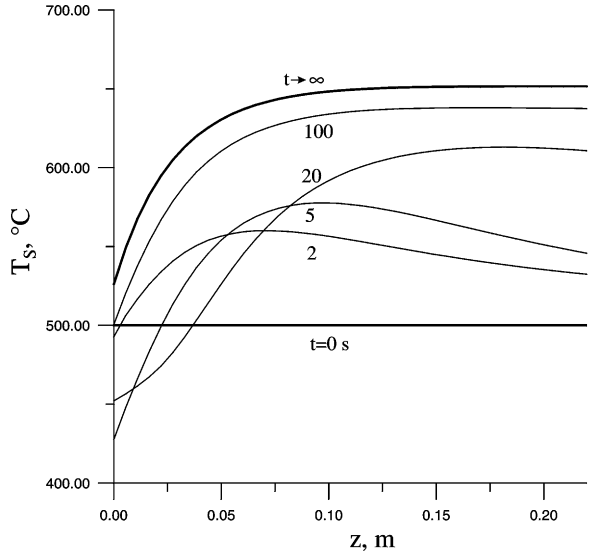

Fig. 9. Dynamic evolution of the axial solid temperature profile during a start-up procedure. $T_i = 500°C$, $\lambda = 0.7$, $T_f = 20°C$ and $y_{Af} = 0.025$.

5.2. Dynamic analysis of start-up procedures for Design II

Fig. 9 shows the dynamic evolution of the axial solid temperature profile during a start-up procedure. At the beginning of the process the solid is supposed to be at a constant temperature of 500°C, and a cold reactants mixture (at 20°C) enters the reactor. At these conditions the solid phase has enough energy to preheat the reactants during the transient period. The solid temperature near the reactor inlet decreases during the first seconds because the solid matrix acts as a gas preheater. During this period the outlet gas temperature increases and therefore the value of T_0 starts to rise (caused by a hotter recycle) from 20°C ($t = 0$ s) to around 430°C ($t = 20$ s). Then, the solid temperature near the reactor inlet begins to increase. After 100 s the reactor is close to reach its final steady state (point A of Fig. 6).

Fig. 10 presents the solid temperature dynamics if the initial solid temperature (T_i) is lower than the minimum value required to ignite the system. Although the solid temperature becomes higher than T_i in the second half of the reactor during a short period of time, the initial energy stored by the solid is not enough to avoid the extinction of the reaction.

The outlet methane conversion as a function of time is shown in Fig. 11 for three different initial solid temperatures. As it can be seen, for $T_i = 500°C$ and 450°C the conversion values are very close to the unity after a short initial period of time. This behavior indicates that just for few seconds unburned methane is released to the atmosphere (after 0.5 s the outlet conversion becomes higher than 80%). For both cases the system evolves towards the same final steady state (point A of Fig. 6), however a longer transient period and a more oscillating response

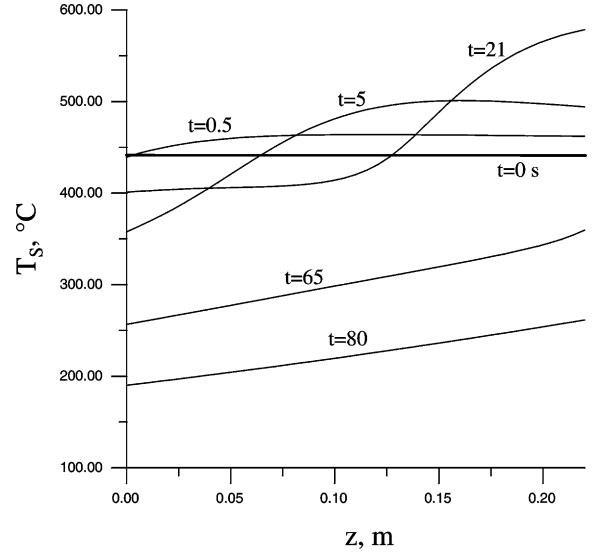

Fig. 10. Dynamic evolution of the axial solid temperature profile during a start-up procedure. $T_i = 442.5°C$, $\lambda = 0.7$, $T_f = 20°C$ and $y_{Af} = 0.025$.

is observed for $T_i = 450°C$. Finally, for $T_i = 442.5°C$ the reaction extinguishes after around 70 s.

6. Conclusions

Steady-state and dynamic results have demonstrated that autothermal catalytic units, after an appropriate start-up procedure, can operate with high methane conversion, without exceeding the maximum allowable

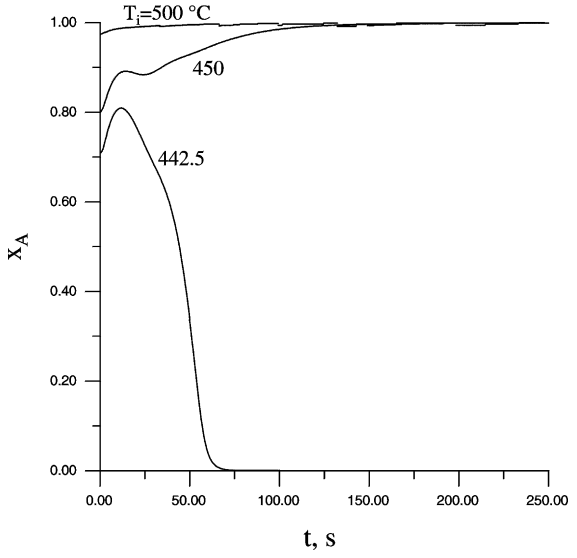

Fig. 11. Dynamic evolution of the outlet conversion for different T_i ($\lambda = 0.7$, $T_f = 20°C$, $y_{Af} = 0.025$).

temperature and minimizing harmful emissions such as NO_x (to preheat the reactants, the flame of the conventional units is replaced by the heat feedback of a fraction of the total heat generated by the catalytic reaction).

Due to the dilution originated by the recycle stream (which admits the use of higher y_{Af}) and for the same process constraints, Design II appears as the most convenient alternative because it can provide significantly higher heat fluxes than Design I. Moreover, Design II can provide an exit stream at the highest thermal level (for a given maximum allowable temperature) feasible for an autothermal converter.

To operate with high conversion and dynamic stability, the operating conditions for Design II lie in a region where multiple steady states occur (e.g., around point A of Fig. 6). However, start-up procedures based on an initial heating of the solid matrix up to temperatures around 450–500°C allow to reach steady states of high conversion after a short transient period. For a selected set of operating conditions (point A of Fig. 6), dynamic studies have demonstrated that the proposed steady state is stable for disturbances of practical interest.

In order to preheat the reactants mixture Design I requires a gas–gas heat exchanger with large area, because of the low heat transfer coefficients. Despite the need of a device to recycle a fraction of the exhaust gases, Design II is expected to be smaller and simpler than Design I.

A monolithic structure with recycle appears as a suitable alternative to design an autothermal catalytic combustor for hot gas generation, capable to operate at flameless conditions and low contaminant emissions.

References

Briot, P., & Primet, M. (1991). Catalytic oxidation of methane over palladium supported on alumina. *Applied Catalysis*, *68*, 301–314.

Chaouki, J., Guy, C., Sapundzhiev, C., Kusohorsky, D., & Klvana, D. (1994). Combustion of methane in a cyclic catalytic reactor. *I&EC Research*, *33*(12), 2957–2963.

Cybulski, A., & Moulijn, J. A. (1994). Monoliths in heterogeneous catalysis. *Catalysis Reviews in Science and Engineering, 36*(2), 179–270.

Cybulski, A., & Moulijn, J. A. (1998). *Structured catalysts and Reactors*. New York: Marcel Deker Inc.

Groppi, G., Tronconi, E., & Forzatti, P. (1993). Modelling of catalytic combustors for gas turbine applications. *Catalysis Today*, *17*, 237–250.

Hawthorn, R. D. (1974). Afterburner catalysis — effects of heat and mass transfer between gas and catalyst surface. Shell Development Co., Report, 2121, Emeryville, USA. *AIChE Symposium Series*, *70*(137), 428–438.

Hayes, R. E., Kolaczkowski, S. T., Thomas, W. J., & Titiloye, J. (1996). Transient experiments and modeling of the catalytic combustion of methane in a monolith reactor. *Industrial and Engineering Chemistry Research*, *35*(2), 406–414.

Hayes, R. E., & Kolaczkowski, S. T. (1997). *Introduction to Catalytic Combustion*. Amsterdam: Gordon and Breach Sci. Pub.

Irandoust, S., Andersson, B. (1988). Monolithic catalysts for nonautomobile applications. *Catalysis Reviews in Science and Engineering, 30*(3), 341–392.

Kirchner, T., & Eigenberger, G. (1997). On the dynamic behavior of automotive catalysts. *Catalysis Today*, *38*, 3–12.

Kolaczkowski, S. T., Thomas, W. J., Titiloye, J., & Worth, D. J. (1996). Catalytic combustion of methane in a monolith reactor: Heat and mass transfer under laminar flow and pseudo-steady-state reactions conditions. *Combustion Science and Technology*, *118*, 79–100.

Leung, D., Hayes, R. E., & Kolaczkowski, S. T. (1996). Diffusion limitation effects in the washcoat of a catalytic monolith reactor. *Canadian Journal of Chemical Engineering*, *74*, 94–103.

Ribeiro, F. H., Chow, M., & Dalla Betta, R. A. (1993). Kinetics of the complete oxidation of methane over supported palladium catalysts. *Journal of Catalysis*, *146*, 537–544.